

A First-Principles Study on the Chemisorption of Arsenic on the Cellulose Biopolymer

Art Anthony Z. Munio^{1,2,*}, Diamond C. Domato¹, Alvanh Alem G. Pido³, Yhebron J. Lagud^{4,5}, Leo Cristobal C. Ambolode II^{1,6}

¹ Physics Department, Mindanao State University – Iligan Institute of Technology, A. Bonifacio Avenue, 9200 Iligan City, Philippines

² College of Arts and Sciences, Jose Rizal Memorial State University, Gov. Guading Adaza Street, 7120 Dapitan City, Zamboanga del Norte, Philippines

³ Physics Department, Mindanao State University – Main Campus, 9700 Marawi City, Philippines

⁴ College of Engineering, Jose Rizal Memorial State University, Gov. Guading Adaza Street, 7120 Dapitan City, Zamboanga del Norte, Philippines

⁵ College of Agriculture and Forestry, Jose Rizal Memorial State University, Gov. Guading Adaza Street, 7120 Dapitan City, Zamboanga del Norte, Philippines

⁶ Premier Research Institute of Science and Mathematics (PRISM), Mindanao State University – Iligan Institute of Technology, A. Bonifacio Avenue, 9200 Iligan City, Philippines

* Correspondence: artanthony.munio@g.msuiit.edu.ph;

Received: 30.11.2022; Accepted: 12.01.2023; Published: 26.03.2023

Abstract: Here, we provide fundamental insights on the atomic Arsenic (As) adsorption on the cellulose biopolymer using first-principles density functional theory. The findings indicate that the adsorption process is exothermic in nature, where the As can spontaneously adsorb on different sites of cellulose. The calculated binding energy shows that the As strongly interacts with the hydroxyl and hydroxymethyl group of the cellulose and is minimal on the cellulose's backbone. In all studied configurations, As gained an electronic charge in all four reactive sites and revealed the localization of electrons in the interface of As and cellulose. The electronic band structure shows that the impurity states of the As appear near the Fermi level, thus lowering the bandgap of the cellulose-As systems. Further, the optical absorption spectra of cellulose-As systems revealed new peaks at the visible region. These results suggest cellulose biopolymer can be used as an adsorbent and sensing material for As.

Keywords: cellulose biopolymer; arsenic; adsorption; density functional theory; electronic structure; absorption spectra; sensor.

© 2023 by the authors. This article is an open-access article distributed under the terms and conditions of the Creative Commons Attribution (CC BY) license (<https://creativecommons.org/licenses/by/4.0/>).

1. Introduction

The rise of global industrialization leads to unexpected environmental contamination with hazardous inorganic chemicals [1]. Often, freshwater sources and aquatic organisms are seriously affected, which can lead to catastrophic environmental effects. Arsenic (As) is one of the most hazardous inorganic chemicals released in water systems from factories, industries, and electronic and agricultural waste [2]. Severe As effects on human health involve various types of cancer, immunological system disorders, cognitive deficits, and others [3]. Moreover, some places worldwide have more As deposits in soil and groundwater, a significant factor in As contamination [4]. Hence, accurately assessing of As level in the environment is crucial before it can contaminate living organisms and lead to human consumption. Thus, various research efforts were dedicated to removing and detecting As from freshwater sources [5–8].

Most adsorbent materials that remove As are activated carbon, metal-oxides, and alumina [9–11]. Despite their reported effectiveness, these materials can further create secondary contamination, which is equally dangerous [12]. A more eco-friendly and effective adsorbent material is more attractive for this particular reason. In the recent past, cellulose biopolymers have been studied to remove heavy metal ions, toxic dyes, salts, and oils [13–17]. The effectiveness of cellulose biopolymers is reflected in the number of scientific reports and patents of cellulose for water remediation technology [18–20]. Various reports show cellulose-based materials are promising for removing heavy metal compounds in water [12,13,21–24]. The fundamental understanding of the adsorption of heavy metals on the cellulose biopolymer is a prerequisite in designing effective adsorbent material. Despite its importance, limited studies examine the interaction of heavy metals and biopolymers at the fundamental level [25,26].

Herein, we explain in detail the adsorption mechanism of the neutral As atom on the cellulose biopolymer. The density functional theory (DFT) is utilized for the entire calculations, which is proven to be an indispensable method for studying chemical interaction [25,27–29]. The charge density difference, charge transfer, electronic band structure, and optical absorption spectra of cellulose-As systems are calculated to obtain the perspicacity of the chemical interaction. The findings indicate that the As is strongly adsorbed on the cellulose's hydroxyl and hydroxymethyl group, and a relatively weaker interaction is observed on the cellulose's backbone. The adsorption of As leads to the appearance of impurity states near the Fermi level, thus lowering the cellulose bandgap of cellulose-As systems. These new impurity states cause new peaks in the visible region of the optical absorption spectra. The change in cellulose's bandgap and optical response upon adsorption of As is a valuable criterion for sensing As. These results provide new information as a reference for future works on biopolymer and heavy metals systems.

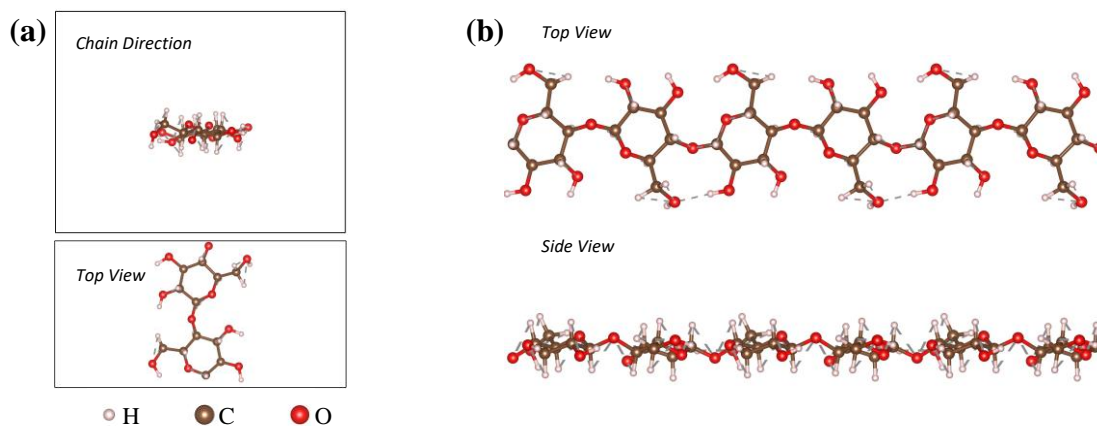


Figure 1. (a) The simulation box of cellulose used in the calculations and (b) the corresponding $1 \times 1 \times 3$ supercell of the cellulose biopolymer.

2. Materials and Methods

All DFT calculations are carried out using Quantum Espresso within generalized gradient approximation (PBE parametrization), Optimized Norm-Conserving Vanderbilt Pseudopotential, plane-wave basis set, and Grimme-D3 dispersion correction [30–33]. The energy and charge cutoff is set to the standard value, 60Ry, and 240 Ry, respectively. The optimization calculation sets the energy and force threshold to 10^{-6} Ry and 10^{-5} Ry /Bohr, respectively. A $1 \times 1 \times 5$ k-points centered at the Γ -point are used in the optimization calculations.

There are 30 k-points used to estimate the electronic band structure of the studied systems sampled between Γ and Z high symmetry points. The dielectric constant of the studied systems is calculated using Random Phase Approximation (RPA) with 143 bands considered implemented in the *epsilon* post-processing tool of Quantum Espresso.

3. Results and Discussion

The optimized configuration of cellulose and the simulation box is displayed in Figure 1a, and its corresponding supercell is shown in Figure 1b. The vacuum slab is included to isolate the cellulose chain and avoid the long-range effect of van der Waals force between periodic images of the biopolymer. The dimension of the simulation box is 21 Å x 16 Å x 10.49 Å. The length of the cellulose is obtained by performing variable cell optimization, ensuring that the cellulose chain is not under stress in the z-direction. The resulting length agrees with the reported cellobiose in crystal form (~10.38 Å) [34,35]. The minor difference in the unit length is attributed to the chemical environment and the intrinsic limitation of both DFT calculations and experimental methods. The calculated bandgap of cellulose is ~ 4.98 eV, which agrees with the experimental and theoretical reports [36,37]. This further verifies that DFT within PBE level theory can provide useful information for studying cellulose biopolymers and other natural polymers [25,36,38].

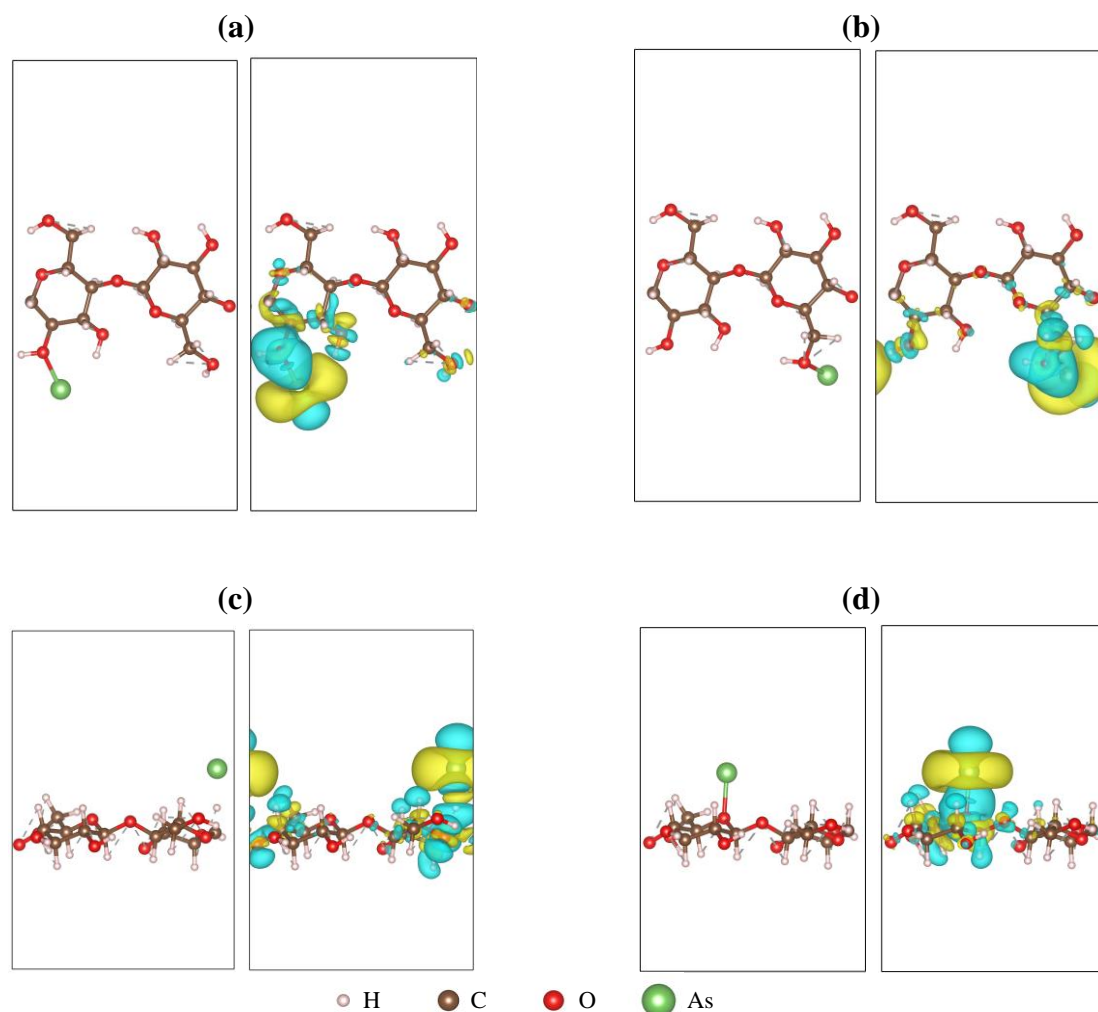


Figure 2. The cellulose chain's optimized structure (left) and the corresponding charge density difference (right) with adsorbed As in four sites. The As is near the (a) hydroxyl group and (b) hydroxymethyl group of the cellulose. (c)-(d) the As is placed in the cellulose's backbone. The accumulation and depletion of the electronic charge are denoted by yellow and cyan isosurface, respectively.

There are four sites studied for the adsorption of As. In Figure 2a and Figure 2b, the initial placement of the As is in the vicinity of the hydroxyl and hydroxymethyl groups, respectively. The binding energy in these regions (Figure 2a and Figure 2b) are -1.07 eV and -0.92 eV, respectively. There is relatively lower binding energy when the As is at the cellulose's backbone regions, as shown in Figures 2c (-0.34 eV) and 2d (-0.67). Although these results indicate that cellulose can be utilized to trap As, a lower magnitude of binding energy suggests that As can quickly diffuse if enough energy is gained.

Aside from calculating the binding energy and the interaction distance, electronic distribution is also crucial for the non-trivial differentiation of chemical interaction [39–41]. The corresponding charge redistribution is visualized by calculating the charge density difference shown in the right panel in Figure 2. Generally, Figure 2a-Figure 2d revealed that the depletion of electronic charge is mainly at the cellulose chain and accumulates towards the As region. Using Bader charge transfer analysis, the As in Figure 2a, Figure 2b, Figure 2c, and Figure 2d accumulate 0.045 e, 0.035 e, 0.153 e, and 0.046 e, respectively.

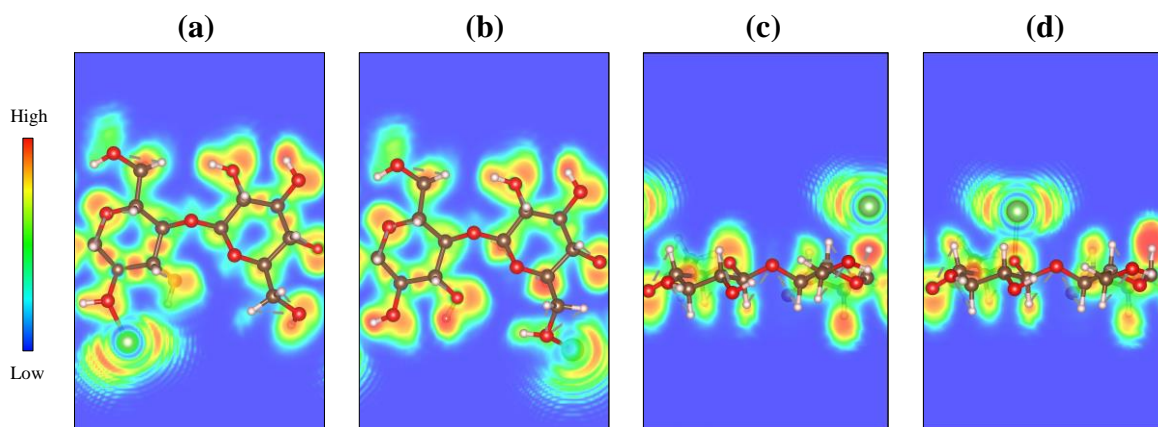


Figure 3. The 2D-ELF of cellulose-As systems. The As atom adsorbed on (a) hydroxyl group, (b) hydroxymethyl group, and (c)-(d) cellulose's backbone.

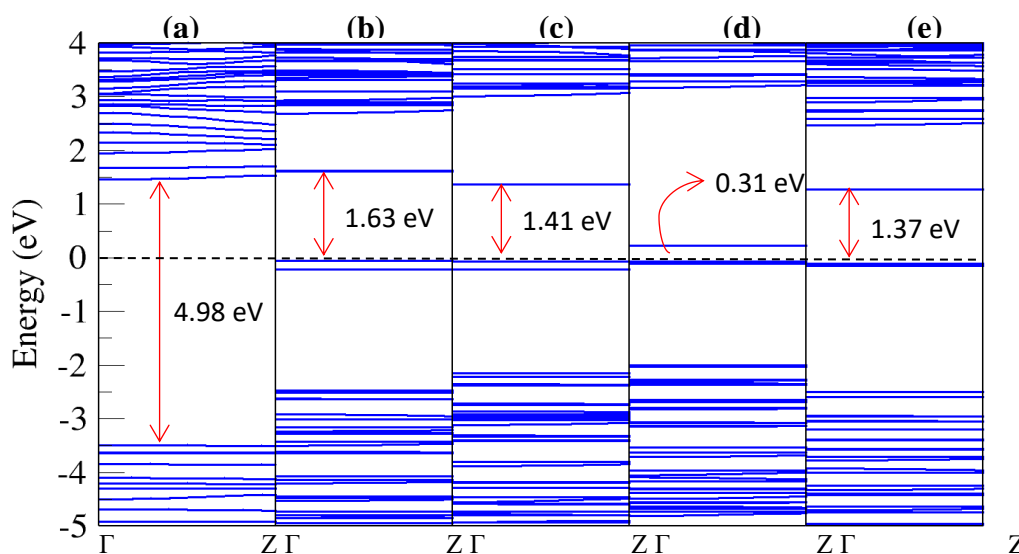


Figure 4. The electronic band structure of the studied configurations was calculated from $\Gamma - Z$ k-path. (a) Isolated cellulose has a wide bandgap of 4.98 eV. Cellulose-As configurations, the adsorption sites of As are near the (b) hydroxyl group, (c) hydroxymethyl group, (d) cellulose's backbone in Fig.2c, and (e) cellulose's backbone in Fig.2d.

The electron localization function (ELF) is further calculated to examine the topology of electronic localization further to distinguish between chemical or physical bonding [39]. Red to yellow ELF basin indicates highly localized electrons interpreted as a lone pair or strong chemical bonding. Metallic bonding is depicted by yellow to cyan ELF basins. Figure 3a-Figure 3d illustrates sharing of electrons indicated by faint green ELF basins at the interface of As and cellulose. This type of interaction is similar to metallic-organic interaction [39].

Table 1. Summary of interaction distance, binding energy, charge transfer, and bandgap of cellulose-As systems.

Configuration	Bonding	Interaction Distance (Å)	Binding Energy (eV)	¹ Charge Transfer (e)	Bandgap (eV)
Fig.2a – Site 1	O-As	2.06	-1.07	0.045	1.63
Fig.2b – Site 2	O-As	2.07	-0.77	0.035	1.41
Fig.2c – Site 3	H-As	1.89	-0.35	0.153	0.31
Fig.2d – Site 4	O-As	2.12	-0.66	0.046	1.37

¹Gain of electronic charge of As.

The electronic band structure of cellulose with adsorbed As in all sites is displayed in Figure 3. Note that the Fermi level is taken as the reference. The flat bands and wide bandgap nature of cellulose are evident in Figure 4a, verifying its insulating property [36]. The adsorption of As on the cellulose creates impurity states near the Fermi level, thus, reducing the bandgap of cellulose-As systems. The bandgap is related to the conductivity and absorbance spectra of material; hence it can be the basis for sensing adsorbed foreign chemicals. The relevant information relating to the cellulose-As systems is summarized in Table 1.

The absorbance spectra of cellulose and cellulose-As systems are displayed in Figure 5a (0 eV to 15 eV) and Figure 5b (0 eV to 6 eV).

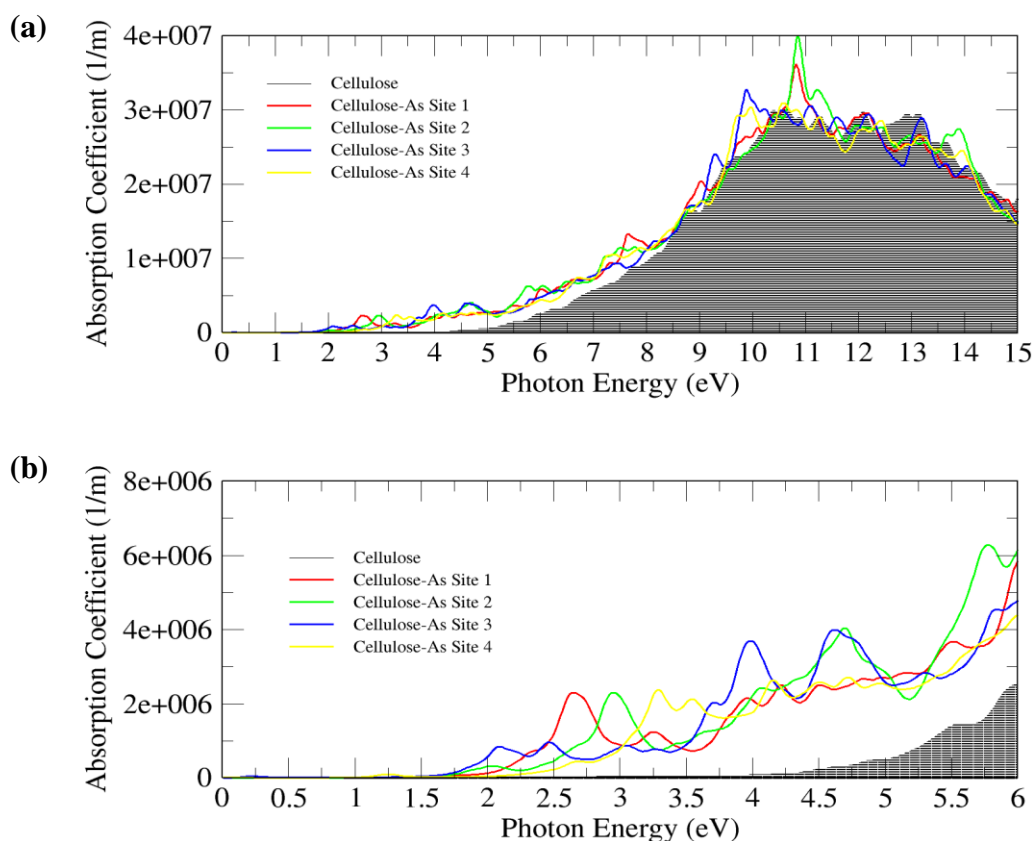


Figure 5. The absorption spectra of the cellulose-As systems in the photon energy range of (a) 0 eV – 15 eV and (b) 0 eV – 6 eV.

The absorption spectrum (dropped black lines) in Figure 5a and Figure 5b shows cellulose absorbing light near its bandgap energy (~ 4.98 eV) in the UV region in agreement with experimental findings [42]. A drastic increase in the absorbance coefficient is observed from ~ 5 eV to ~ 10 eV of the cellulose. It should be noted that the absorbance coefficient in higher photon energy (>10 eV) is greatly affected by the number of bands included in the dielectric constant calculations. Thus, trends in this region should be interpreted carefully. In Figure 5b, the absorbance spectrum of cellulose with adsorbed As appears to have shifted to the lower photon energy. The shift of absorption spectra is due to the reduction of bandgap and realignment of energy levels shown in Figure 4b-Figure 4e. The general trends in the absorbance spectrum of the cellulose are reproduced in the cellulose-As systems in photon energy > 5 eV, except for the appearance of new sharp absorption peaks. Since the findings demonstrate significant modification of the cellulose optical response on exposure to atomic As, we anticipate the results here open the possibility of a cellulose-based optical sensor for the detection of atomic As. This can be a valuable reference for identifying the optical fingerprint of atomic As on cellulose.

The findings discussed here supports experimental results in removing heavy metals using cellulose-based material [43–48]. It is known that As(III) and As(V) are the usual oxidation state of As in water, so many experiments are dedicated to this. For example, Tian et al.[49] shows that arsenic compounds in the form of AsO_4^{3-} and AsO_2^- can be efficiently adsorbed on the modified cellulose. Ciopec et al.[50] provide an assessment of As(V) removal using activated cellulose fibers. The finding indicates that the adsorption is chemical, based on the calculated activation energy. Their result is in agreement with our findings presented here. Generally, the main advantage of cellulose-based as an adsorbent is its large surface area, multiple active adsorption sites, and susceptibility to chemical transformation.

Overall, the DFT calculation demonstrates that cellulose can be utilized for trapping and sensing As. The main reason for the success of cellulose as adsorbent material for As is due to its many active sites. The results presented here provide fundamental insights into the interaction of the As with the cellulose biopolymer. It should be noted, however, As exist in various compound forms. Thus, further study on the interaction of the As compounds should be evaluated to obtain a solid conclusion and explain experimental findings. Moreover, the solution effect on the interaction of the cellulose was not considered, which is necessary for an accurate description of interactions. Nevertheless, the results discussed provide fundamental trends and the nature of the interaction of cellulose and As systems, bridging the literature gap.

4. Conclusions

The adsorption of the neutral As on the cellulose biopolymer is systematically assessed using first-principles DFT with Grimme-D3 dispersion. The optimized atomic configuration of cellulose-As systems indicates that the As can spontaneously adsorb in various sites of the cellulose. Stronger interaction is observed when the As bonded with the hydroxyl and hydroxymethyl groups and is minimal in the cellulose's backbone. These results are verified by performing the Bader charge transfer analysis and examining the redistribution of the electrons. The results yield solid evidence that cellulose is effective as renewable adsorbent material for trapping As. It is further found that the adsorption of As creates impurity states near the Fermi level, lowering the bandgap of the cellulose-As systems. The reduced bandgap allows the cellulose-As systems to absorb light in the visible region. These significant changes in the electronic bandgap and optical absorbance spectra can be considered a fingerprint for As

adsorption. The obtained results provide a fundamental understanding of the bonding mechanism of As with cellulose biopolymer. This study will reference future works on cellulose-based adsorbent materials to remove heavy metals from fresh water.

Funding

This research received support from Jose Rizal Memorial State University through the project "Exploring the Adsorption of Heavy Metal Compounds on Nanocellulose and Nanocarbons: A First-principles Study".

Acknowledgments

The authors acknowledge the support of the Republic of the Philippines.

Conflicts of Interest

The authors declare no conflict of interest.

References

1. Ahmed, S.F.; Kumar, P.S.; Rozbu, M.R.; Chowdhury, A.T.; Nuzhat, S.; Rafa, N.; Mahlia, T.M.I.; Ong, H.C.; Mofijur, M. Heavy Metal Toxicity, Sources, and Remediation Techniques for Contaminated Water and Soil. *Environmental Technology & Innovation* **2022**, *25*, 102114, <https://doi.org/10.1016/j.eti.2021.102114>.
2. Garelick, H.; Jones, H.; Dybowska, A.; Valsami-Jones, E. Arsenic Pollution Sources. *Rev Environ Contam Toxicol* **2008**, *197*, 17–60, https://doi.org/10.1007/978-0-387-79284-2_2.
3. Singh, R.; Singh, S.; Parihar, P.; Singh, V.P.; Prasad, S.M. Arsenic Contamination, Consequences and Remediation Techniques: A Review. *Ecotoxicology and Environmental Safety* **2015**, *112*, 247–270, <https://doi.org/10.1016/j.ecoenv.2014.10.009>.
4. Shankar, S.; Shanker, U.; Shikha, U. Arsenic Contamination of Groundwater: A Review of Sources, Prevalence, Health Risks, and Strategies for Mitigation. *The Scientific World Journal* **2014**, *2014*, e304524, <https://doi.org/10.1155/2014/304524>.
5. Abdelhamid, H.N.; Georgouvelas, D.; Edlund, U.; Mathew, A.P. CelloZIFPaper: Cellulose-ZIF Hybrid Paper for Heavy Metal Removal and Electrochemical Sensing. *Chemical Engineering Journal* **2022**, *446*, 136614, <https://doi.org/10.1016/j.cej.2022.136614>.
6. Xia, L.; Feng, H.; Zhang, Q.; Luo, X.; Fei, P.; Li, F. Centrifugal Spinning of Lignin Amine/Cellulose Acetate Nanofiber for Heavy Metal Ion Adsorption. *Fibers Polym* **2022**, *23*, 77–85, <https://doi.org/10.1007/s12221-021-3210-0>.
7. Nakakubo, K.; Endo, M.; Sakai, Y.; Biswas, F.B.; Wong, K.H.; Mashio, A.S.; Taniguchi, T.; Nishimura, T.; Maeda, K.; Hasegawa, H. Cross-Linked Dithiocarbamate-Modified Cellulose with Enhanced Thermal Stability and Dispersibility as a Sorbent for Arsenite Removal. *Chemosphere* **2022**, *307*, 135671, <https://doi.org/10.1016/j.chemosphere.2022.135671>.
8. Kundu, R.; Mahada, P.; Chhirang, B.; Das, B. Cellulose Hydrogels: Green and Sustainable Soft Biomaterials. *Current Research in Green and Sustainable Chemistry* **2022**, *5*, 100252, <https://doi.org/10.1016/j.crgsc.2021.100252>.
9. Rafique, M.; Hajra, S.; Tahir, M.B.; Gillani, S.S.A.; Irshad, M. A Review on Sources of Heavy Metals, Their Toxicity and Removal Technique Using Physico-Chemical Processes from Wastewater. *Environ Sci Pollut Res* **2022**, *29*, 16772–16781, <https://doi.org/10.1007/s11356-022-18638-9>.
10. Zhang, W.; Cho, Y.; Vithanage, M.; Shaheen, S.M.; Rinklebe, J.; Alessi, D.S.; Hou, C.-H.; Hashimoto, Y.; Withana, P.A.; Ok, Y.S. Arsenic Removal from Water and Soils Using Pristine and Modified Biochars. *Biochar* **2022**, *4*, 55, <https://doi.org/10.1007/s42773-022-00181-y>.
11. Yin, C.; Li, S.; Liu, L.; Huang, Q.; Zhu, G.; Yang, X.; Wang, S. Structure-Tunable Trivalent Fe-Al-Based Bimetallic Organic Frameworks for Arsenic Removal from Contaminated Water. *Journal of Molecular Liquids* **2022**, *346*, 117101, <https://doi.org/10.1016/j.molliq.2021.117101>.
12. Chen, H.; Sharma, S.K.; Sharma, P.R.; Yeh, H.; Johnson, K.; Hsiao, B.S. Arsenic(III) Removal by Nanostructured Dialdehyde Cellulose–Cysteine Microscale and Nanoscale Fibers. *ACS Omega* **2019**, *4*, 22008–22020, <https://doi.org/10.1021/acsomega.9b03078>.
13. Ahankari, S.; George, T.; Subhedar, A.; Kar, K.K. Nanocellulose as a Sustainable Material for Water Purification. *SPE Polymers* **2020**, *1*, 69–80, <https://doi.org/10.1002/pls2.10019>.

14. Chen, Y.; Yang, G.; Liu, B.; Kong, H.; Xiong, Z.; Guo, L.; Wei, G. Biomineralization of ZrO₂ Nanoparticles on Graphene Oxide-Supported Peptide/Cellulose Binary Nanofibrous Membranes for High-Performance Removal of Fluoride Ions. *Chemical Engineering Journal* **2022**, *430*, 132721, <https://doi.org/10.1016/j.cej.2021.132721>.
15. Ajala, O.J.; Khadir, A.; Ighalo, J.O.; Umenweke, G.C. Chapter 17 - Cellulose-Based Nano-Biosorbents in Water Purification. In *Nano-Biosorbents for Decontamination of Water, Air, and Soil Pollution*; Denizli, A., Ali, N., Bilal, M., Khan, A., Nguyen, T.A., Eds.; Micro and Nano Technologies; Elsevier, 2022; pp. 395–415 ISBN 978-0-323-90912-9, <https://www.elsevier.com/books/nano-biosorbents-for-decontamination-of-water-air-and-soil-pollution/denizli/978-0-323-90912-9>.
16. Abdelhamid, H.; P Mathew, A. Cellulose-Based Materials for Water Remediation: Adsorption, Catalysis, and Antifouling. *Frontiers in Chemical Engineering* **2021**, *3*, 790314, <https://doi.org/10.3389/fceng.2021.790314>.
17. Abdelhamid, H.N.; Mathew, A.P. Cellulose–Metal Organic Frameworks (CelloMOFs) Hybrid Materials and Their Multifaceted Applications: A Review. *Coordination Chemistry Reviews* **2022**, *451*, 214263, <https://doi.org/10.1016/j.ccr.2021.214263>.
18. Fan, J.; Zhang, S.; Li, F.; Shi, J. Cellulose-Based Sensors for Metal Ions Detection. *Cellulose* **2020**, *27*, 5477–5507, <https://doi.org/10.1007/s10570-020-03158-x>.
19. Aziz, T.; Farid, A.; Haq, F.; Kiran, M.; Ullah, A.; Zhang, K.; Li, C.; Ghazanfar, S.; Sun, H.; Ullah, R.; et al. A Review on the Modification of Cellulose and Its Applications. *Polymers* **2022**, *14*, 3206, <https://doi.org/10.3390/polym14153206>.
20. Hamidon, T.S.; Adnan, R.; Haafiz, M.K.M.; Hussin, M.H. Cellulose-Based Beads for the Adsorptive Removal of Wastewater Effluents: A Review. *Environ Chem Lett* **2022**, *20*, 1965–2017, <https://doi.org/10.1007/s10311-022-01401-4>.
21. Najib, N.; Christodoulatos, C. Removal of Arsenic Using Functionalized Cellulose Nanofibrils from Aqueous Solutions. *Journal of Hazardous Materials* **2019**, *367*, 256–266, <https://doi.org/10.1016/j.jhazmat.2018.12.067>.
22. Mosaferi, M.; Nemati, S.; Khataee, A.; Nasseri, S.; Hashemi, A.A. Removal of Arsenic (III, V) from Aqueous Solution by Nanoscale Zero-Valent Iron Stabilized with Starch and Carboxymethyl Cellulose. *J Environ Health Sci Eng* **2014**, *12*, 74, <https://doi.org/10.1186/2052-336X-12-74>.
23. Tewatia, P.; Kumar, V.; Samota, S.; Singhal, S.; Kaushik, A. Sensing and Annihilation of Ultra-Trace Level Arsenic (III) Using Fluoranthene Decorated Fluorescent Nanofibrous Cellulose Probe. *Journal of Hazardous Materials* **2022**, *424*, 127722, <https://doi.org/10.1016/j.jhazmat.2021.127722>.
24. Kaur, J.; Sengupta, P.; Mukhopadhyay, S. Critical Review of Bioadsorption on Modified Cellulose and Removal of Divalent Heavy Metals (Cd, Pb, and Cu). *Ind. Eng. Chem. Res.* **2022**, *61*, 1921–1954, <https://doi.org/10.1021/acs.iecr.1c04583>.
25. Ezzat, H.; Anter, A.; Omara, W.; Basyouni, O.; Helmy, S.; Mohamed, A.; Tawfik, Prof.W. Dft: B3lyp/Lanl2dz Study for the Removal of Fe, Ni, Cu, as, Cd and Pb with Chitosan. *Biointerface Research in Applied Chemistry* **2020**, *10*, <https://doi.org/10.33263/BRIAC106.70027010>.
26. Reis, D.T.; Ribeiro, I.H.S.; Pereira, D.H. DFT Study of the Application of Polymers Cellulose and Cellulose Acetate for Adsorption of Metal Ions (Cd²⁺, Cu²⁺ and Cr³⁺) Potentially Toxic. *Polym. Bull.* **2020**, *77*, 3443–3456, <https://doi.org/10.1007/s00289-019-02926-5>.
27. Shtepliuk, I.; Caffrey, N.M.; Iakimov, T.; Khranovskyy, V.; Abrikosov, I.A.; Yakimova, R. On the Interaction of Toxic Heavy Metals (Cd, Hg, Pb) with Graphene Quantum Dots and Infinite Graphene. *Sci Rep* **2017**, *7*, 3934, <https://doi.org/10.1038/s41598-017-04339-8>.
28. Svetlana, J.; Marković, Z.; Ngo, C.; Dao, D.Q. Insight into Interaction Properties between Mercury and Lead Cations with Chitosan and Chitin: Density Functional Theory Studies. *Computational and Theoretical Chemistry* **2018**, *1138*, 99–106, <https://doi.org/10.1016/j.comptc.2018.06.010>.
29. Zhang, Y.; Zhao, Y.; Yang, Y.; Liu, P.; Liu, J.; Zhang, J. DFT Study on Hg⁰ Adsorption over Graphene Oxide Decorated by Transition Metals (Zn, Cu and Ni). *Applied Surface Science* **2020**, *525*, 146519, <https://doi.org/10.1016/j.apsusc.2020.146519>.
30. Giannozzi, P.; Baroni, S.; Bonini, N.; Calandra, M.; Car, R.; Cavazzoni, C.; Ceresoli, D.; Chiarotti, G.L.; Cococcioni, M.; Dabo, I.; et al. QUANTUM ESPRESSO: A Modular and Open-Source Software Project for Quantum Simulations of Materials. *J Phys Condens Matter* **2009**, *21*, 395502, <https://doi.org/10.1088/0953-8984/21/39/395502>.
31. Giannozzi, P.; Baseggio, O.; Bonfà, P.; Brunato, D.; Car, R.; Carnimeo, I.; Cavazzoni, C.; de Gironcoli, S.; Delugas, P.; Ferrari Ruffino, F.; et al. Quantum ESPRESSO toward the Exascale. *J. Chem. Phys.* **2020**, *152*, 154105, <https://doi.org/10.1063/5.0005082>.
32. Prandini, G.; Marrazzo, A.; Castelli, I.E.; Mounet, N.; Marzari, N. A Standard Solid State Pseudopotentials (SSSP) Library Optimized for Precision and Efficiency (Version 1.0, Data Download); **2018**, <https://doi.org/10.24435/materialscloud:2018.0001/v2>.
33. Grimme, S.; Antony, J.; Ehrlich, S.; Krieg, H. A Consistent and Accurate Ab Initio Parametrization of Density Functional Dispersion Correction (DFT-D) for the 94 Elements H-Pu. *J. Chem. Phys.* **2010**, *132*, 154104, <https://doi.org/10.1063/1.3382344>.

34. Nishiyama, Y.; Sugiyama, J.; Chanzy, H.; Langan, P. Crystal Structure and Hydrogen Bonding System in Cellulose I(Alpha) from Synchrotron X-Ray and Neutron Fiber Diffraction. *J Am Chem Soc* **2003**, *125*, 14300–14306, <https://doi.org/10.1021/ja037055w>.
35. Nishiyama, Y.; Langan, P.; Chanzy, H. Crystal Structure and Hydrogen-Bonding System in Cellulose I β from Synchrotron X-Ray and Neutron Fiber Diffraction. *J. Am. Chem. Soc.* **2002**, *124*, 9074–9082, <https://doi.org/10.1021/ja0257319>.
36. Srivastava, D.; Kuklin, M.S.; Ahopelto, J.; Karttunen, A.J. Electronic Band Structures of Pristine and Chemically Modified Cellulose Allomorphs. *Carbohydrate Polymers* **2020**, *243*, 116440, <https://doi.org/10.1016/j.carbpol.2020.116440>.
37. Simao, C.; Reparaz, S.; Wagner, M.; Graczykowski, B.; Kreuzer, M.; Ruiz-Blanco, Y.; Garcia, Y.; Malho, J.-M.; Goñi, A.; Ahopelto, J.; et al. Optical and Mechanical Properties of Nanofibrillated Cellulose: Toward a Robust Platform for next-Generation Green Technologies. *Carbohydrate Polymers* **2015**, *126*, <https://doi.org/10.1016/j.carbpol.2015.03.032>.
38. Omer, A.M.; Dey, R.; Eltaweil, A.S.; Abd El-Monaem, E.M.; Ziora, Z.M. Insights into Recent Advances of Chitosan-Based Adsorbents for Sustainable Removal of Heavy Metals and Anions. *Arabian Journal of Chemistry* **2022**, *15*, 103543, <https://doi.org/10.1016/j.arabjc.2021.103543>.
39. Koumpouras, K.; Larsson, J.A. Distinguishing between Chemical Bonding and Physical Binding Using Electron Localization Function (ELF). *J. Phys.: Condens. Matter* **2020**, *32*, 315502, <https://doi.org/10.1088/1361-648X/ab7fd8>.
40. Henkelman, G.; Arnaldsson, A.; Jónsson, H. A Fast and Robust Algorithm for Bader Decomposition of Charge Density. *Computational Materials Science* **2006**, *36*, 354–360, <https://doi.org/10.1016/j.commatsci.2005.04.010>.
41. Jiao, Y.; Ma, F.; Zhang, X.; Heine, T. A Perfect Match between Borophene and Aluminium in the AlB₃ Heterostructure with Covalent Al–B Bonds, Multiple Dirac Points and a High Fermi Velocity. *Chemical Science* **2022**, *13*, 1016–1022, <https://doi.org/10.1039/D1SC05207A>.
42. Orelma, H.; Hokkanen, A.; Leppänen, I.; Kammiovirta, K.; Kapulainen, M.; Harlin, A. Optical Cellulose Fiber Made from Regenerated Cellulose and Cellulose Acetate for Water Sensor Applications. *Cellulose* **2020**, *27*, <https://doi.org/10.1007/s10570-019-02882-3>.
43. Tian, Y.; Wu, M.; Liu, R.; Li, Y.; Wang, D.; Tan, J.; Wu, R.; Huang, Y. Electrospun Membrane of Cellulose Acetate for Heavy Metal Ion Adsorption in Water Treatment. *Carbohydrate Polymers* **2011**, *83*, 743–748, <https://doi.org/10.1016/j.carbpol.2010.08.054>.
44. Zhang, M.; Zhang, L.; Tian, H.; Lu, A. Universal Preparation of Cellulose-Based Colorimetric Sensor for Heavy Metal Ion Detection. *Carbohydrate Polymers* **2020**, *236*, 116037, <https://doi.org/10.1016/j.carbpol.2020.116037>.
45. Fakhre, N.A.; Ibrahim, B.M. The Use of New Chemically Modified Cellulose for Heavy Metal Ion Adsorption. *Journal of Hazardous Materials* **2018**, *343*, 324–331, <https://doi.org/10.1016/j.jhazmat.2017.08.043>.
46. Sheikhzadeh, E.; Naji-Tabasi, S.; Verdian, A.; Kolahi-Ahari, S. Equipment-Free and Visual Detection of Pb²⁺ Ion Based on Curcumin-Modified Bacterial Cellulose Nanofiber. *J IRAN CHEM SOC* **2022**, *19*, 283–290, <https://doi.org/10.1007/s13738-021-02305-w>.
47. Low, S.C.; Azmi, N.A. binti; Ong, C.S.; Lim, J.K. Environmental Monitoring of Trace Metal Pollutants Using Cellulosic-Paper Incorporating Color Change of Azo-Chromophore. *Environ Sci Pollut Res* **2022**, *29*, 71614–71631, <https://doi.org/10.1007/s11356-022-20706-z>.
48. Magar, H.S.; Magd, E.E.A.-E.; Hassan, R.Y.A.; Fahim, A.M. Rapid Impedimetric Detection of Cadmium Ions Using Nanocellulose/Ligand/Nanocomposite (CNT/Co₃O₄). *Microchemical Journal* **2022**, *182*, 107885, <https://doi.org/10.1016/j.microc.2022.107885>.
49. Tian, Y.; Wu, M.; Liu, R.; Wang, D.; Lin, X.; Liu, W.; Ma, L.; Li, Y.; Huang, Y. Modified Native Cellulose Fibers—A Novel Efficient Adsorbent for Both Fluoride and Arsenic. *Journal of Hazardous Materials* **2011**, *185*, 93–100, <https://doi.org/10.1016/j.jhazmat.2010.09.001>.
50. Ciopec, M.; Biliuta, G.; Negrea, A.; Duțeanu, N.; Coseri, S.; Negrea, P.; Ghangrekar, M. Testing of Chemically Activated Cellulose Fibers as Adsorbents for Treatment of Arsenic Contaminated Water. *Materials* **2021**, *14*, 3731, <https://doi.org/10.3390/ma14133731>.